DOI: 10.1002/ejic.200501045

# Kinetic and Thermodynamic Aspects of the CT and T-Shaped Adduct Formation Between 1,3-Dimethylimidazoline-2-thione (or -2-selone) and Halogens

M. Carla Aragoni,[a] Massimiliano Arca,[a] Francesco A. Devillanova,*[a] Patrizio Grimaldi,*[b] Francesco Isaia,[a] Francesco Lelj,*[b] and Vito Lippolis[a]

**Keywords:** Density functional calculations / Donor–acceptor systems / Hypervalent compounds / Selenium / Sulfur

The reactions between L=E donors [L: 1,3-dimethylimidazolyl framework; E: S (**1**), Se (**2**)] and halogens $X_2$ (X: Cl, Br, I) to form either "T-shaped" hypervalent chalcogen (TY) or linear charge-transfer-type adducts (CT) have been studied in the density functional theory (DFT) context by considering both thermodynamic and kinetic aspects. Apart from the case of the adducts between sulfur donors and diiodine, hypervalent compounds are calculated to be always more stable than CT ones in the gas phase, in agreement with the experimental results based on spectroscopic and structural determinations. NBO and FMO analyses suggest explanations for this. Reaction mechanism studies reveal that CT adducts are always the first products of the reactions and no transition states connecting the reactants directly to TY adducts have been found. The present calculations indicate that, at least for **1** and **2**, TY adducts are obtained from CT adducts and not directly from the reactants.



## Introduction

The reactions between chalcogenone donors (L=E; L: organic framework; E: S, Se) and $X_2$ halogen molecules (X: Cl, Br, I) continue to attract a great deal of interest in the scientific community due to their implication in numerous and different fields of research, which span from synthetic and supramolecular aspects to biological, materials, and industrial chemistry.[1–10] In particular, in the last ten years we have reported[4] the isolation of several classes of compounds from the reactions of thio- and selenoketone donors with halogens. In fact, besides charge transfer (CT) and T-shaped (TY) adducts, which bear linear E–X–X and X–E–X groups, respectively, donor oxidation products with chalcogen–halogen terminal bonds (L–E–X), linear two-coordinate halogen (I) atoms with chalcogen ligands ([LE–X–EL]$^+$), and dications containing a chalcogen–chalcogen single bond ([$(LE)_2$]$^{2+}$) represent some of the most common types of products characterised by X-ray crystallography. In many cases, a very small change in the chemical environment of the donor or the experimental conditions is enough to produce each of the above-mentioned products.[8] Therefore, an important goal in this field is the complete understanding of all possible pathways that allow for the interconversion between the various species in equilibrium.

The first general qualitative criterion that can be used to foresee the formation of CT or TY adducts was based on the electronegativity values of the halogen and the chalcogen: the formation of TY adducts prevails if the electronegativity value of the halogen is higher than that of the chalcogen atom, while CT adducts prevail if the reverse is true.[2] However, a more general attempt to explain the formation of the various types of compounds obtainable by reacting L=E donors with halogens has been made by Husebye and co-workers,[3] who proposed a chemical scheme according to which the [LEX]$^+$ cation plays a central role in determining the different pathways of the reactions and the nature of the final products. This cation might originate from either the CT adduct or from the TY adduct by heterolytic cleavage of the X–X or E–X bond, respectively.

Recently, the central role of the cation [LEX]$^+$ in the formation of the various products has been tested on a series of different L=E donors on the basis of DFT calculations.[4h] In particular, the NBO charge distribution calculated for the hypothetical cationic species allowed the prediction of the preferential formation of CT or TY adducts when X is Br or I. In addition, a criterion was proposed to draw-up an order of ability to form the dicationic species ([L–E–E–L]$^{2+}$) for the considered L=E donors. This criterion suggested imidazoline-2-thione to be the top-ranking sulfur donor in the ability to form these dications, as sub-

[a] Dipartimento di Chimica Inorganica ed Analitica, Università di Cagliari, S.S. 554,
Bivio per Sestu, 09042 Monserrato (CA), Italy
E-mail: devilla@vaxca1.unica.it
[b] LaMI Dipartimento di Chimica and LaSCaMM-INSTM Sezione Basilicata, Università della Basilicata,
Via N. Sauro, 85100 Potenza, Italy
E-mail: grimaldi@unibas.it
lelj@unibas.it

  

sequently observed experimentally.[7] On the basis of these encouraging results, we decided to use DFT calculations in order to achieve further insight into the origin of the relative stability of the various products and to explore the possibility of interconversion among the various species in solution. In fact, this seemed very important in order to clarify the whole reaction mechanism and test the hypothesis of Husebye from a computational point of view. A first problem to clarify was whether it is always necessary to hypothesize the formation of the $[LEX]^+$ cation as an intermediate or whether there are other accessible reaction pathways that lead to formation of the final products.

The most general reactivity scheme of L=E donors with halogens or inter-halogens in forming CT and TY adducts is depicted in Scheme 1.

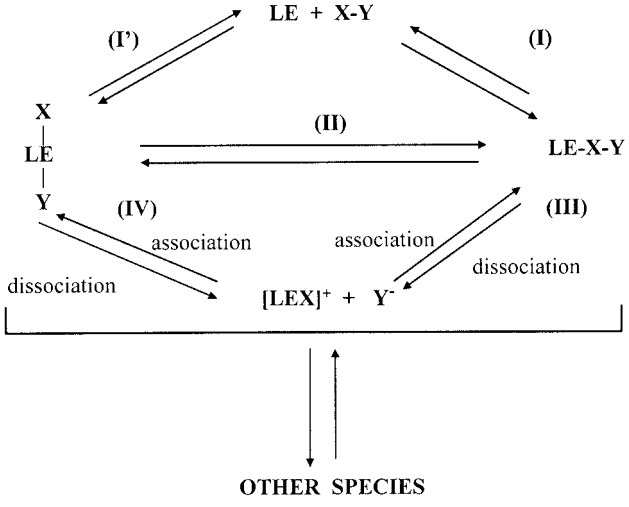


Scheme 1. General scheme for the reactivity of LE donors with halogen (X equal to Y) and interhalogen molecules (X not equal to Y), involving only the CT and TY adducts and the $[LEX^+]$ cation.

In the present study we discuss the mechanistic aspects with respect to non-ionic species also, addressing our attention to the kinetic and thermodynamic aspects of the formation of CT and TY adducts (pathways I′ and I of Figure 1) by direct attack of an $X_2$ molecule (X: Cl, Br or I) on 1,3-dimethylimidazoline-2-thione (**1**) and -2-selone (**2**) (see Scheme 2), and on the possible interconversion between these adducts (pathway II).

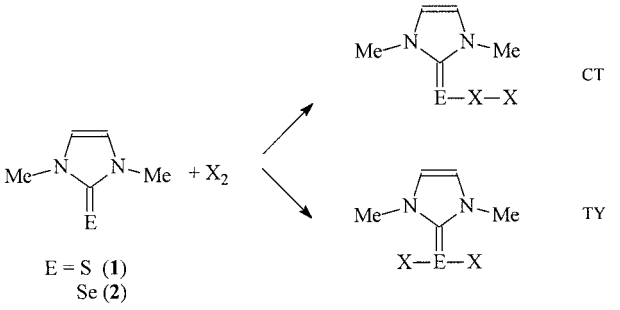


Scheme 2. The two donors and the two possible products (CT and TY adducts) of the interaction between the imidazoline donors and $X_2$.

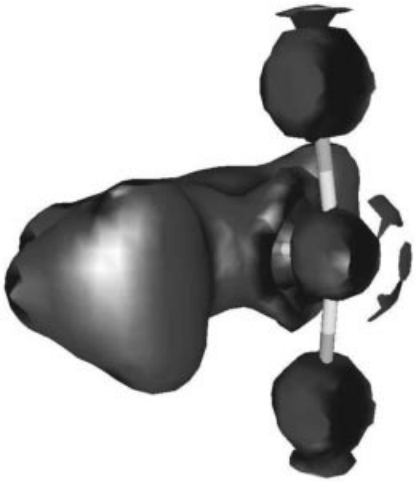

Figure 1. $\nabla^2\rho$ computed for **1**·$Br_2$ using MP2 density showing a charge concentration on the outer side of the chalcogen atom.

## Computational Methods and Search Techniques for Transition States

DFT and MP2[11] calculations were performed on an Alpha workstation using the Gaussian 98 (rev. A7 and A11) program and the implemented version of the NBO (natural bond orbital) analysis program.[12,13] The geometries of the adducts were fully optimised at the DFT level. In our previous DFT calculations on the TY adducts,[4h,4j] we used the hybrid B3LYP functional,[14] the Schafer, Horn and Ahlrichs[15] basis sets for C, H, N, O, S and Se, and the LANL2DZ basis sets together with effective core potentials (ECP)[16] for halogen atoms. The geometries of the CT and TY halogen adducts of 1,3-dimethylimidazoline-2-thione (**1**) and 1,3-dimethylimidazoline-2-selone (**2**) were therefore optimised at the same level of theory. In order to evaluate the influence of the model on the optimisations, CT and TY $Br_2$ adducts of **1** and **2** were also optimised at the MP2 and DFT with an asymptotic corrected hybrid functional[17] level with the Schafer, Huber and Ahlrichs basis sets.[18] $Br_2$ adducts were been chosen because it is possible to use a basis set without pseudo-potentials and because of the intermediate position of Br between Cl and I. In both cases the results showed no significant differences with respect to those obtained with the other model. The transition states of the reactions between **1** and **2** and halogens $X_2$ (X: I, Br, Cl) were localised by the NEPR (negative eigenvalues progressive reduction) technique.[19]

Since it has been observed[20] that the DFT approach can give incorrect indications about the structures and energies of transition states of closed-shell interacting fragments, we have also performed some MP2 calculations on the potential energy surface (PES) of selected reactants (**1** and $Br_2$) towards the CT isomer. The relative stabilities of the CT and TY adducts in the gas phase were analysed according to the NBO method.[13] NBO analysis is based on a method for optimally transforming a given wavefunction into its

  

localised form, corresponding to the one-centre (lone pair) or two-centre (bond) functions. Delocalisation effects appear as weak departures from this idealised localised picture. The energetic importance of these effects can be estimated according to a second-order perturbation theory approach. Since these delocalisation effects lead to loss of occupancy from the localised NBO (σ, π or lone pair) of the idealised Lewis structure into the empty non-Lewis, antibonding (σ* or π*) and Rydberg (R*) orbitals, and thus to departures from the idealised Lewis structure description, they are referred to as "delocalisation" corrections to the zeroth-order Lewis structure. For each donor NBO (*i*) and acceptor NBO (*j*), the stabilisation energy ($\Delta E_{ij}$) associated with delocalisation $i \rightarrow j$ is estimated as $\Delta E_{ij} = q_i \cdot [F(i,j)^2]/(\varepsilon_j - \varepsilon_i)$, where $q_i$ is the donor orbital occupancy, $\varepsilon_j$ and $\varepsilon_i$ are the diagonal elements (orbital energies) and F(*i*,*j*) is the off-diagonal NBO Fock matrix element (see ref.[13] for a detailed discussion).

## Results and Discussion

### Relative Stability of Isomers: Optimisations, NBO and FMO Analysis

Table 1 reports some relevant optimised geometrical parameters together with available experimental data of the CT and TY adducts of **1** and **2**. The agreement is very good and, furthermore, it is worthy to note that for TY adducts the method is able to account for the small deviations of the angle X–E–X from 180°, as observed for **2**·$I_2$ and other related adducts.[4h–4k,8,9] Analysis of $\nabla\rho^2$[22] suggests an explanation for this deviation (see Figure 1). According to the $\nabla\rho^2$ values there is a charge accumulation near the chalcogen on the outer side of the adduct that bends the two halogen atoms towards the molecular ring. DFT calculations indicate that hypervalent compounds for both **1** and **2** are thermodynamically favoured with respect to the CT isomers in all but the case of **1**·$I_2$ (see Table 2). The energy difference between CT and TY adducts decreases as the halogen atomic number increases and the chalcogen one reduces.

Table 2. Calculated stability [kcal mol$^{-1}$] of the CT with respect to the TY isomers (taken as 0.0) for **1** and **2**.

| | **1** | **2** |
|---|---|---|
| $Cl_2$ | 11.5 | 21.3 |
| $Br_2$ | 2.1 | 10.6 |
| $I_2$ | –3.7 | 3.5 |

In the cases of **1**·$Cl_2$, **2**·$Cl_2$, and **2**·$Br_2$ the TY adduct formation is clearly preferred, whereas in the cases of **1**·$Br_2$, **1**·$I_2$ and **2**·$I_2$ the energy differences between the two types of adducts are so small (<4 kcal mol$^{-1}$) that the experimental trend in the stability of the possible isomers can be modified by environmental effects. However, it should be remembered that no CT adducts between thioketonic donors and $Br_2$ or TY adducts with $I_2$ have been characterised so far. This relative order of stability does not change when using different approximations both in basis set and in the level of approximations.

Figure 2 reports the HOMO–1 and HOMO energies of **1** and **2** and the LUMO energies of the $X_2$ molecules. As can be seen, the HOMO energy of **1** is lower than the LUMO energy of $I_2$ only in the case of the couple **1**/$I_2$, and only in this case is the CT adduct thermodynamically favoured with respect to the TY one. It is also interesting to observe that there is a linear relationship between the NBO charges on the chalcogen atom E of the TY adducts and the frontier molecular orbital $(HOMO–1)_{LE}$ – $(LUMO)_{X_2}$ energy difference (see Figure 3).

In fact, Figure 2 shows that $(HOMO–1)_{LE}$ – $(LUMO)_{X_2}$ is lower than the $(HOMO)_{LE}$ – $(LUMO)_{X_2}$ energy difference in all cases, the exception being the case of **1**·$I_2$. Moreover, the HOMO–1 is mainly a p orbital on the chalcogen, whereas the HOMO has a non-negligible delocalisation on the imidazoline ring. This makes the interaction of dihalogen LUMOs with $(HOMO–1)_{LE}$ more relevant than the interaction with $(HOMO)_{LE}$.

Table 1. Relevant geometrical parameters of the optimised geometries of CT and TY adducts of **1** and **2** (X: halogen, E: chalcogen; distances in angstroms and angles in degrees). The structural data available for related compounds are reported in parentheses.

| TY Adducts | **1**·$Cl_2$ | **2**·$Cl_2$ | **1**·$Br_2$ | **1**·$Br_2$[a] | **1**·$Br_2$[4h],[b,c] | **2**·$Br_2$[4k],[d] | **1**·$I_2$ | **2**·$I_2$[8] |
|---|---|---|---|---|---|---|---|---|
| X–E | 2.53 | 2.59 | 2.71 | 2.54 | 2.53 (2.49) | 2.77 (2.66, 2.52) | 2.91 | 2.98 (2.74, 2.89) |
| E–C | 1.78 | 1.90 | 1.78 | 1.73 | 1.73 (1.75) | 1.90 (1.95) | 1.78 | 1.89 (1.89) |
| X–E–X | 170.64 | 170.17 | 171.95 | 168.41 | 170.59 (179.38) | 170.76 (175.7) | 175.70 | 170.24 (178.64) |
| X–E–C–N | 102.30 | 109.15 | 95.06 | 90.01 | 90.09 (76.0) | 102.84 (–101 to 78) | 90.00 | 89.93 (–94.4 to 90.0) |
| **CT Adducts** | **1**·$Cl_2$ | **2**·$Cl_2$ | **1**·$Br_2$ | **1**·$Br_2$[a] | **1**·$Br_2$[b] | **2**·$Br_2$ | **1**·$I_2$[41],[e] | **2**·$I_2$[8],[e] |
| X–X | 2.40 | 2.43 | 2.66 | 2.45 | 2.44 | 2.69 | 3.01 (2.90) | 3.03 (2.99, 2.91) |
| X–E | 2.66 | 2.72 | 2.80 | 2.73 | 2.73 | 2.89 | 2.99 (2.68) | 3.09 (2.72, 2.78) |
| E–C | 1.74 | 1.87 | 1.74 | 1.69 | 1.69 | 1.87 | 1.74 (1.72) | 1.87 (1.88, 1.86) |
| X–X–E | 176.81 | 175.95 | 178.12 | 176.69 | 178.70 | 178.13 | 178.46 (175.7) | 178.37 (176.86, 175.63) |
| X–E–C | 91.94 | 89.88 | 94.45 | 85.83 | 93.56 | 92.34 | 96.64 (96.8) | 93.59 (93.0, 96.9) |
| X–E–C–N | 111.21 | 115.85 | 106.98 | 88.55 | 109.48 | 111.42 | 104.07 (–96.4 to 84.4) | 108.63 (–100.4 to 84.6) |

[a] MP2 calculations. [b] DFT with asymptotic corrected hybrid functional. [c] Structural data refer to *N*,*N*′-dimethylbenzoimidazole-2-ylium dibromosulfanide. [d] Structural data refer to 1,2-bis(3-methyl-4-imidazolin-2-ylium dibromoselenanide)ethane. [e] Structural data refer to 1,1′-bis(3-methyl-4-imidazolin-2-chalcogenone)methane bis(diiodine).

  

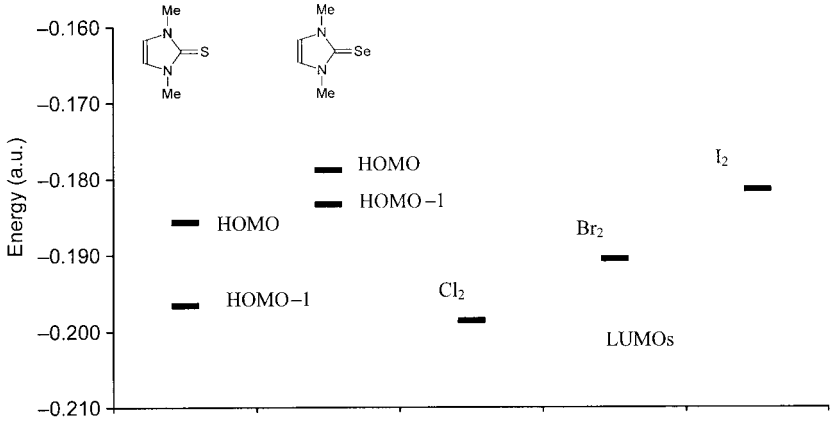


Figure 2. Calculated KS orbital energy of the HOMOs and HOMO–1s of **1** and **2**, and of LUMOs of the halogens $X_2$.

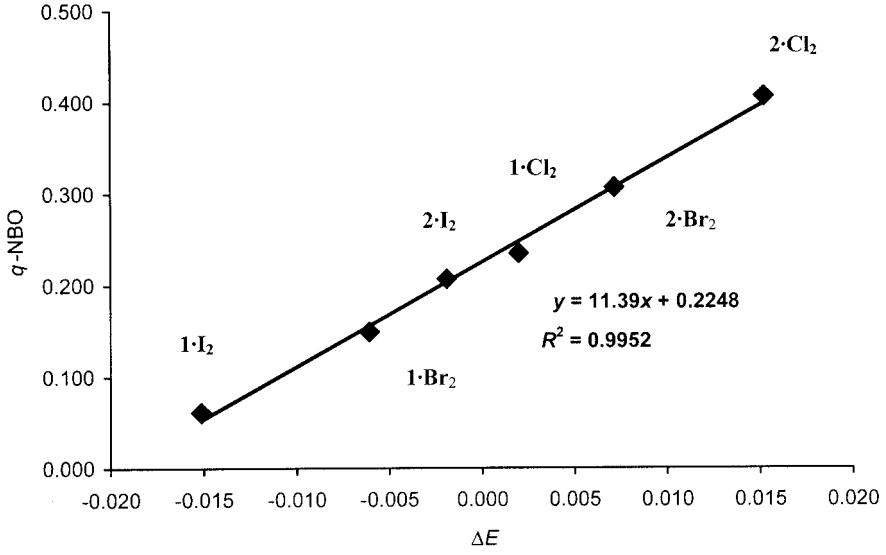


Figure 3. NBO net charges on the chalcogen (E) atoms of the TY adducts between **1** and **2** with the halogen $X_2$ as a function of the energy difference between $(HOMO–1)_{LE}$ and $(LUMO)_{X_2}$.

To gain a deeper insight into the relative stability of TY and CT adducts, an NBO energetic analysis was performed on all the compounds at the B3LYP/(SV-LanL2DZ) level by assigning the electrons in order to obtain two closed-shell fragments: a halide anion, $X^-$, and the remaining $[LEX]^+$ cation. The interaction of $X^-$ either with the chalcogen atom or with the halogen atom of the $[LEX]^+$ cation formally accounts for the formation of the TY and CT adducts, respectively. We must stress, however, that this scheme does not suggest any underlying reaction mechanism but is simply a useful approach that allows us to compare the origin of the stability in the two isomers (CT and TY) with respect to the same reference fragments.

The NBO energetic analysis (see Table 3) and the particular choice of the interacting fragments allow us not only to quantify the energy contribution of the charge transfer from the halide anion to the cation (column e in Table 3) but also to account for the contributions of the polarisation effects within the $[LEX]^+$ fragment. As an example, the NBO orbitals that contribute most to the relative stabilities of the TY adduct **1**·$Br_2$ are depicted in Figure 4.

For all the adducts examined the excitation processes within the $[LEX]^+$ cation involve two-centre localised bond orbitals (σ) and a one-centre valence lone pair (lp) orbital as donors and higher energy empty orbitals (σ*, π* and R*) that can behave as acceptors and, subsequently, as donors. In the interaction between the two fragments, two of the numerous delocalisation contributions are found to be the most relevant ones (see Table 3 and Figure 4). The first of these is due to an intramolecular polarisation effect and involves the reorganisation of the electronic structure of the cation due to the presence of the anion. This reorganisation can be described by two intra-cation charge-transfer processes, one from a carbon–chalcogen bonding orbital to a carbon–nitrogen antibonding orbital, which occurs through two intermediate orbitals: a carbon–chalcogen antibonding and a carbon Rydberg orbital (see columns a–c of Table 3), and the other involving a relatively small back-donation

  

Table 3. NBO energetic analysis results. Columns a–d are relative to the intrafragment polarisation effects. Column e concerns the interfragment charge transfer. All data are in kcal mol$^{-1}$.

| | Intramolecular polarisation effects | | | | Total polarisation effect contributions | Charge transfer |
|---|---|---|---|---|---|---|
| Adducts/Orbitals | *a* $\sigma_{(C-E)} \rightarrow \pi^*_{(C-E)}$ | *b* $\pi^*_{(C-E)} \rightarrow R^*_C$ | *c* $R^*_C \rightarrow \sigma^*_{(C-N)}$ | *d* $\sigma_{(C-N)} \rightarrow \pi^*_{(C-E)}$ | (*a*+*b*+*c*+*d*) $\sigma_{(C-E)} \rightarrow \sigma^*_{(C-N)}$ $\sigma_{(C-N)} \rightarrow \pi^*_{(C-E)}$ | *e* $lp_X \rightarrow \sigma^*_{(E-X)}$ |
| 1·$Cl_2$ (TY) | 1.9 | 45.0 | 45.0 | 5.0 | 96.9 | 48.0 |
| 1·$Cl_2$ (CT) | 5.3 | 14.0 | 0.45 | 3.0 | 22.7 | 110.0 |
| 2·$Cl_2$ (TY) | 3.0 | 20.0 | 50.0 | 12.0 | 85.0 | 45.0 |
| 2·$Cl_2$ (CT) | 6.0 | 11.0 | 0.45 | 5.0 | 22.4 | 90.0 |
| 1·$Br_2$ (TY) | 0.7 | 182.0 | 80.0 | 28.0 | 290.7 | 48.0 |
| 1·$Br_2$ (CT) | 2.0 | 110. | 120. | 13.0 | 245.0 | 92.0 |
| 2·$Br_2$ (TY) | 1.6 | 30.0 | 40.0 | 10.0 | 81.6 | 45.0 |
| 2·$Br_2$ (CT) | 5.0 | 12.0 | 45.0 | 5.0 | 22.5 | 95.0 |
| 1·$I_2$ (TY) | 0.5 | 0.7 | 45 | 37.0 | 83.2 | 48.0 |
| 1·$I_2$ (CT) | 0.6 | 30.0 | 0.5 | 7.0 | 38.1 | 100.0 |
| 2·$I_2$ (TY) | 0.45 | 300.0 | 50.0 | 13.0 | 363.4 | 30.0 |
| 2·$I_2$ (CT) | 40.0 | 250.0 | 0.5 | 1.5 | 292.0 | 97.0 |

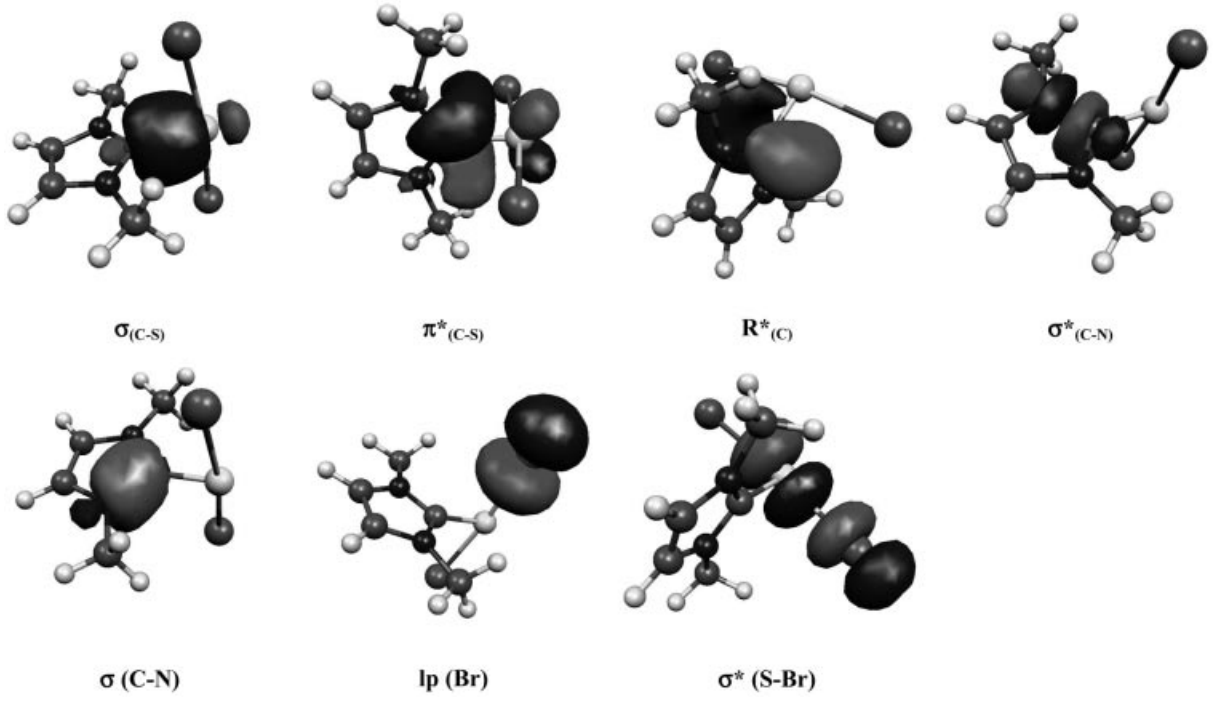


Figure 4. NBO localised orbitals calculated for **1**·$Br_2$ involved in the polarisation effects (see Table 3).

from carbon–nitrogen bonding orbitals to carbon–chalcogen antibonding orbitals (see column d of Table 3). The second is an inter-fragment process that involves the two $[LEX]^+$ and $X^-$ fragments. It is a strong charge-transfer from the halide anion lone pair to the halogen–chalcogen σ* orbital.

The sum of the energy stabilisation contributions (Table 3) gives, approximately, the relative stability for every pair of isomers. As can be deduced from this table, the different weight of each contribution determines the energy differences between the CT and TY compounds (see Table 2). In particular, the total polarisation effect contribution in the cation is bigger for the latter compounds, whereas the interfragment charge-transfer prevails in the former.

This approach also allows us to analyse the different behaviour shown by sulfur and selenium derivatives. The NBO analysis shows that the smaller energy difference between **1**·$Cl_2$ adducts (11.5 kcal mol$^{-1}$) with respect to **2**·$Cl_2$ ones (21.3 kcal mol$^{-1}$) is due to a greater stabilisation energy of the charge transfer in the case of the chlorine anion lone pair towards the antibonding S–Cl NBO orbital of the CT adduct. The growing importance of this charge transfer in the selenium CT adducts is the main factor responsible for the smaller energy difference for bromine and iodine compounds with respect to chlorine ones.

  

## Reaction Mechanism

### *Path I*

Scanning the PES for the motion of $X_2$ toward **1** and **2** allowed the identification of putative transition states, although their refinement did not give definite stationary structures in any case. Therefore a deeper investigation was performed in the case of the motion of $Br_2$ toward **1** using different approximations both in the Hamiltonian and in the basis set. DFT with an asymptotic corrected hybrid functional[17] and a post Hartree–Fock perturbative MP2 approach were used. The MP2 approach was used since long-range dispersive interactions need at least a bi-excited configuration contribution. In all cases the Schafer, Horn and Ahlrichs pVDZ[18] basis sets with polarisation functions on all atoms were used in order to better describe polarisation effects. All the models used showed the same Morse-like shape for the total energy, which can be fitted with the Morse function $y = D^*[1 - e^{-\beta(x-x_0)}]^2$ with the following parameters: $\beta$ = 1.3133, $x_0$ = 2.7180 Å and $D$ = 13.5461 kcal mol$^{-1}$ (see Figure 5), thereby excluding the existence of a transition state between reactants and CT adducts. Indeed, the Morse function, starting from a distance $x = x_0 - \beta\ln 2$, always has a negative value of the second derivative with a stationary point at $x = \infty$. This is the reason why, in our opinion, approximately localised putative transition states did not converge to definite transition states but were taken apart to very large distances during the optimisations.

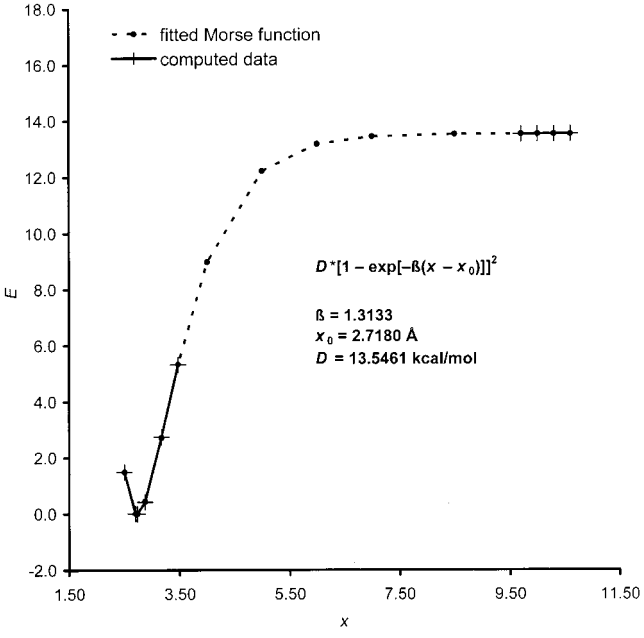


Figure 5. Computed data (in MP2 approximation) and fitted Morse function for the motion of $Br_2$ toward **1**. (energy in kcal mol$^{-1}$ and $x$ in angstroms).

Furthermore, the study of $\nabla^2\rho$[21] allowed us to describe the possible interaction of the two fragments due to electron density. As matter of fact, the $\nabla^2\rho$ (see Figure 6) shows a definite accumulation of the density in an sp shape in front of the chalcogen and a toroidal hole around the π C=E bond in the case of **1**. This can explain the fact that at large distances the interaction is between the "density hole " on the halogen and the charge concentration on the chalcogen, whereas at shorter distances the interaction is on the toroidal hole around the chalcogen and with a spherical charge concentration to even shorter distance in the CT adduct.

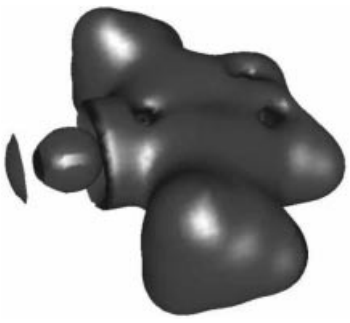

Figure 6. $\nabla^2\rho$ computed for **1** using MP2 density showing a charge concentration in front of the chalcogen atom and a depletion with cylindrical symmetry around the same atom.

### *Path I′ and II*

The six transition states leading to the six TY adducts in the reactions between **1** and **2** with halogens $X_2$ (X: Cl, Br, I) were successfully identified by applying the NEPR technique and confirmed by calculations of the second derivative matrix of the energy with respect to the coordinates. Only one negative eigenvalue was found for each of them, thus confirming the nature of the transition state for the computed structures.

To further confirm the assignment of the transition states to a given reaction path we used the intrinsic reaction coordinate (IRC) approach.[22] This approach allows the connection of each saddle-point to a given reactant/product couple. Indeed, the IRC approach confirmed that the six transition states (of the kind reported in Figure 7) link TY adducts to CT ones but, surprisingly, not to the (LE + $X_2$) reactants. Any further attempt to find a different transition state connecting TY adducts and LE and $X_2$ failed because we always found the same transition state that connected TY and CT adducts. As a consequence of these findings, step I′ of Scheme 1 should be excluded as a possible pathway leading to the TY adduct. Some relevant structural parameters of each optimised transition state are reported in Table 4.

Interestingly, all the six transition states leading to the TY from the CT adducts (see Figure 6) show the halogen molecule occupying the axial and equatorial position of a hypothetical trigonal bipyramid centred on the chalcogen atom. Figure 8 shows the snapshot sequence of the interconversion leading from the CT to the TY adduct through the axial–equatorial transition state. The energy barrier to overcome, with respect to the CT adduct, is in the range 25–40 kcal mol$^{-1}$. In order to evaluate the direct interconversion between the CT and TY adducts (pathway II) of the general Scheme 1 and the paths III and IV

  

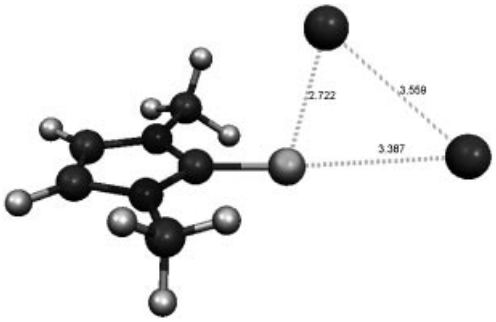


Figure 7. Transition state leading from the CT to the TY adduct in **1**·$I_2$.

Table 4. Relevant geometrical parameters of transition states of TY adducts (distances in angstoms, angles in degreees; X:halogen; E: chalcogen).

| | $E–X_{eq}$ | $E–X_{ax}$ | X–X | X–E–X | $X_{ax}$–E–C–N |
|---|---|---|---|---|---|
| **1**·$Cl_2$ | 2.6 | 2.4 | 3.7 | 97.6 | 81.1 |
| **1**·$Br_2$ | 3.4 | 2.7 | 3.7 | 74.7 | 69.2 |
| **1**·$I_2$ | 3.4 | 2.9 | 4.0 | 76.9 | 71.7 |
| **2**·$Cl_2$ | 3.3 | 2.5 | 4.1 | 89.3 | 111.5 |
| **2**·$Br_2$ | 3.4 | 2.9 | 3.3 | 61.8 | 107.2 |
| **2**·$I_2$ | 3.5 | 3.0 | 3.9 | 72.3 | 64.3 |

through association and dissociation processes, we evaluated the difference between the energy of the transition state leading to the TY from the CT adducts and the energies of the $LEX^+$ and $X^-$ products, which should be lower than the transition state energy of paths III and IV. Our calculation showed that the energies of the $LEX^+$ and $X^-$ ions at infinite distance is of the order of 300 kcal mol$^{-1}$, thus excluding III and IV as possible paths, at least in the gas phase. However, in solvents of high dielectric constant or in the presence of "acid" molecules that can accept the $X^-$ ion (e.g. free $X_2$ molecules), III and IV might compete with the path II. Thus, on the basis of these results it seems very likely that, in the case examined in the present study, the initial product of the interaction between **1** and **2** and $X_2$ is always a linear charge-transfer adduct. In the case of **1** and $I_2$, the CT adduct is the final product of the reaction, otherwise the CT adduct can evolve to the thermodynamically more stable TY adduct. So, although we can't rule out the Husebye hypothesis in polar media, we have shown that a monomolecular process can give rise to the formation of the TY adduct.

## Conclusions

In order to get a deeper insight into the reactions between L=E [L: 1,3-dimethylimidazolyl framework; E: S (**1**), Se (**2**)] and halogens $X_2$ (X: Cl, Br, I), twelve adducts (six of the CT type and six of the TY type) have been theoretically investigated. DFT calculations indicate that, except for the case of **1** and $I_2$, hypervalent adducts (TY) are generally more stable than the linear (CT) ones. Nevertheless, the CT compounds always play an important role in the process as

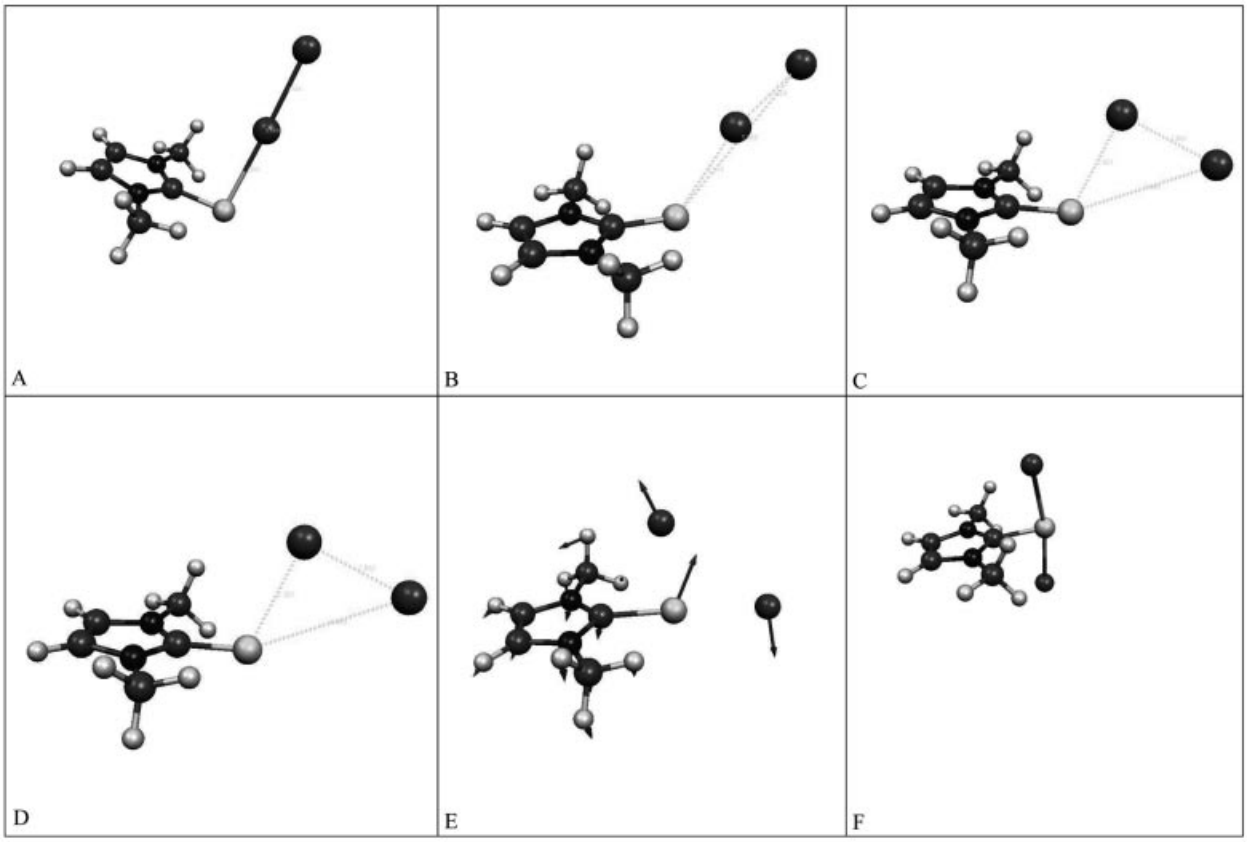


Figure 8. Snapshot sequence from the CT to the TY adduct through an axial–equatorial transition state in **1**·$Br_2$.

  

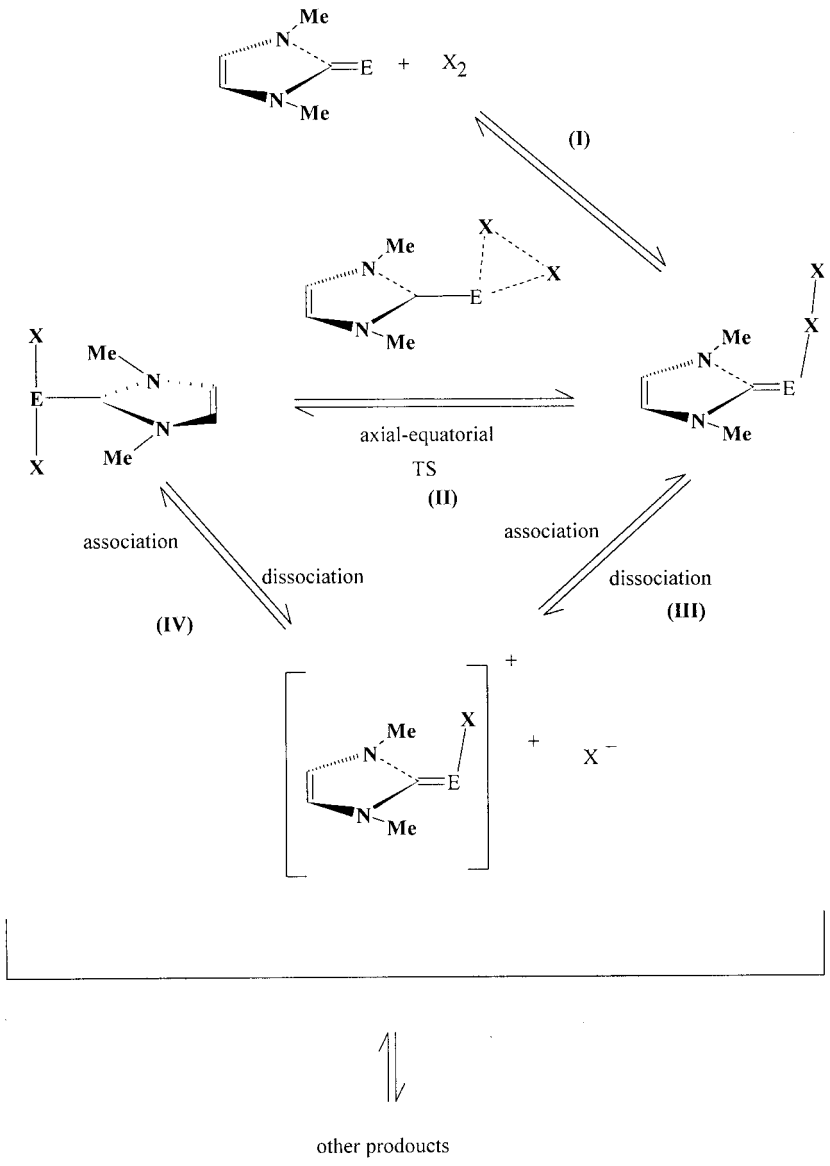


Scheme 3. Reactivity scheme proposed in the present study.

they are always the first product of the reaction from which the TY isomers can be formed through an axial–equatorial transition state.

This study suggests that the supposed formation of the cation $[LEX]^+$ is not always necessary to explain the formation of the TY adducts since the direct interconversion path of the CT to the TY adducts is accessible. In conclusion, on the basis of our calculations we propose the reaction mechanism reported in Scheme 3.

## Acknowledgments

The MIUR Cluster 26 P.O. 8 of legge 488 and MIUR PRIN 2001 and European Union funding through the Regione Basilicata POP 1996-2000 are kindly acknowledged for computational and financial support.

[1] M. C. Baenziger, R. E. Buckles, R. J. Maner, T. D. Simpson, *J. Am. Chem. Soc.* **1969**, *91*, 5749.
[2] W. Nakanishi, S. Hayashi, H. Tukada, H. Iwamura, *J. Phys. Org. Chem.* **1990**, *3*, 358.
[3] M. D. Rudd, S. V. Linderman, S. Husebye, *Acta Chem. Scan.* **1997**, *51*, 689 and references cited therein.
[4] a) M. Arca, F. Demartin, F. A. Devillanova, A. Garau, F. Isaia, V. Lippolis, G. Verani, *J. Chem. Soc., Dalton Trans.* **1999**, 3069; b) F. Demartin, F. A. Devillanova, E. Isaia, V. Lippolis, G. Verani, *Inorg. Chem.* **1993**, *32*, 3694; c) F. Demartin, F. A. Devillanova, A. Garau, F. Isaia, V. Lippolis, G. Verani, *Polyhedron* **1999**, *18*, 3107; d) F. Demartin, F. A. Devillanova, F. Isaia, V. Lippolis, G. Verani, *Inorg. Chim. Acta* **1997**, *255*, 203; e) F. Cristiani, F. A. Devillanova, F. Demartin, F. Isaia, V. Lippolis, G. Verani, *Inorg. Chem.* **1994**, *33*, 6315; f) F. A. Devillanova, P. Deplano, F. Isaia, V. Lippolis, M. L. Mercuri, S. Piludu, G. Verani, F. Demartin, *Polyhedron* **1998**, *7*, 305–312; g) F. Bigoli, E. Demartin, P. Deplano, F. A. Devillanova, F. Isaia, V. Lippolis, M. L. Mercuri, M. A. Pellinghelli, E. E. Trogu, *Inorg.*

  

*Chem.* **1996**, *35*, 3194; h) M. C. Aragoni, M. Arca, F. Demartin, F. A. Devillanova, A. Garau, F. Isaia, F. Lelj, V. Lippolis, G. Verani, *Chem. Eur. J.* **2001**, *7*, 3122 and references cited therein; i) M. Arca, F. A. Devillanova, A. Garau, F. Isaia, V. Lippolis, G. Verani, F. Demartin, *Z. Anorg. Allg. Chem.* **1998**, *624*, 745–749; j) M. C. Aragoni, M. Arca, A. J. Blae, F. A. Devillanova, W.-W. du Mont, A. Garau, F. Isaia, V. Lippolis, G. Verani, C. Wilson, *Angew. Chem. Int. Ed.* **2001**, *40*, 4229; k) F. Bigoli, P. Deplano, F. A. Devillanova, V. Lippolis, M. L. Mercuri, M. A. Pellinghelli, E. F. Trogu, *Eur. J. Inorg. Chem.* **1998**, 137; l) F. Bigoli, P. Deplano, M. L. Mercuri, M. A. Pellinghelli, A. Sabatini, E. F. Trogu, A. Vacca, *J. Chem. Soc., Dalton Trans.* **1996**, 3583.

[5] a) E. Seppala, E. Ruthe, J. Jeske, W.-W. du Mont, P. G. Jones, *Chem. Commun.* **1999**, 1471; b) W.-W. du Mont, *Main Group Chem. News* **1994**, *2*, 18; c) J. Jeske, W.-W. du Mont, P. G. Jones, *Chem. Eur. J.* **1999**, *5*, 385; d) S. Kubiniok, W.-W. du Mont, S. Pohl, W. Saak, *Angew. Chem.* **1988**, *100*, 434; *Angew. Chem. Int. Ed. Engl.* **1988**, *27*, 431; e) W.-W. du Mont, F. Ruthe, *Coord. Chem. Rev.* **1999**, *189*, 101; f) V. Stenzel, J. Jeske, W.-W. du Mont, P. G. Jones, *Inorg. Chem.* **1997**, *36*, 443.

[6] a) P. D. Boyle, W. I. Cross, S. M. Godfrey, C. A. McAuliffe, R. G. Pritchard, S. J. Teat, *J. Chem. Soc., Dalton Trans.* **1999**, 2845; b) S. M. Godfrey, S. L. Jackson, G. A. McAuliffe, R. G. Pritchard, *J. Chem. Soc., Dalton Trans.* **1998**, 4201; c) P. D. Boyle, J. Christie, T. Dyer, S. M. Godfrey, I. R. Howson, C. McArthur, B. Omar, R. G. Pritchard, G. R. Williams, *J. Chem. Soc., Dalton Trans.* **2000**, 3106 and references cited therein.

[7] M. C. Aragoni, M. Arca, F. Demartin, F. A. Devillanova, A. Garau, F. Isaia, V. Lippolis, G. Verani, *J. Am. Chem. Soc.* **2002**, *124*, 4538–4539.

[8] F. Bigoli, A. M. Pellinghelli, P. Deplano, F. A. Devillanova, V. Lippolis, M. L. Mercuri, E. F. Trogu, *Gazz. Chim. It.* **1994**, *124*, 445.

[9] N. Kuhn, T. Kratz, G. Henkel, *Chem. Ber.* **1994**, *127*, 849.

[10] G. L. Abbati, M. C. Aragoni, M. Arca, F. A. Devillanova, A. C. Fabretti, A. Garau, F. Isaia, V. Lippolis, G. Verani, *Dalton Trans.* **2003**, 1515 and references cited therein.

[11] A.Szabo, N. S. Ostlund, in *Modern Quantum Chemistry*, Macmillan Publishing Co. Inc., New York, **1982**.

[12] M. J. Frisch, G. W. Trucks, H. B. Schlegel, G. E. Scuseria, M. A. Robb, J. R. Cheeseman, V. G. Zakrzewski, J. A. Montgomery, R. E. Stratmann, J. C. Burant, S. Dapprich, J. M. Millam, A. D. Daniels, K. N. Kudin, M. C. Strain, O. Farkas, J. Tomasi, V. Barone, M. Cossi, R. Cammi, B. Mennucci, C. Pomelli, C. Adamo, S. Clifford, J. Ochterski, G. A. Petersson, P. Y. Ayala, Q. Cui, K. Morokuma, D. K. Malick, A. D. Rabuck, K. Raghavachari, J. B. Foresman, J. Cioslowski, J. V. Ortiz, B. B. Stefanov, G. Liu, A. Liashenko, P. Piskorz, I. Komaromi, R. Gomperts, R. L. Martin, D. J. Fox, T. Keith, M. A. Al-Laham, C. Y. Peng, A. Nanayakkara, C. Gonzalez, M. Challacombe, P. M. W. Gill, B. G. Johnson, W. Chen, M. W. Wong, J. L. Andres, M. Head-Gordon, E. S. Replogle, J. A. Pople, *Gaussian 98*, Gaussian, Inc. Pittsburgh PA, **1998** (http://www.gaussian.com/).

[13] A. E. Reed, L. A. Curtiss, F. Weinhold, *Chem. Rev.* **1988**, *88*, 899.

[14] a) A. D. Becke, *J. Chem. Phys.* **1993**, *98*, 1372; b) C. Lee, W. Yang, R. G. Parr, *Phys. Rev. B* **1988**, *37*, 785.

[15] A. Schafer, H. Horn, R. Ahlrichs, *J. Chem. Phys.* **1992**, *97*, 2571.

[16] a) P. J. Hay, W. R. Wadt, *J. Chem. Phys.* **1985**, *82*, 270; b) W. R. Wadt, P. J. Hay, *J. Chem. Phys.* **1985**, *82*, 284; c) P. J. Hay, W. R. Wadt, *J. Chem. Phys.* **1985**, *82*, 299.

[17] C. Adamo, V. Barone, *Chem. Phys. Lett.* **1997**, *274*, 242.

[18] A. Schafer, C. Huber, R. Ahlrichs, *J. Chem. Phys.* **1994**, *100*, 5829.

[19] This technique was developed in our laboratory to overcome the problem of the presence of *n*-order saddle points in the research of transition states. In fact, starting from an *n*-order saddle point, the technique allows us to obtain a transition state, i.e. a first-order saddle point, in $n - 1$ optimisation steps.

[20] A. Dreuw, J. L. Weisman, M. Head-Gordon, *J. Chem. Phys.* **2003**, *119*, 2943.

[21] R. F. W. Bader, in *Atoms in Molecules: A Quantum Theory*, Oxford University Press, **1990**.

[22] C. Gonzales, H. B. Schlegel, *J. Chem. Phys.* **1990**, *94*, 5523.

Received: November 23, 2005
Published Online: April 3, 2006

  